CHAPTER IV

RESULTS AND DISSCUSION

4.1 Preparation of the Biosensor

SAMs are often used for immobilization of various bio-components such as cells, proteins and DNA, etc. The carboxylic-terminated alkanethiolate SAM has been often used for immobilization of cells and proteins due to its chemical reactivity with certain chemical groups of the biomolecules (Hui *et al.*, 2005). In this study, Claudin 4 antibodies were immobilized onto alkanethiolate SAM that was formed on a gold electrode. Fig 4.1 shows the illustration of immobilization procedure.
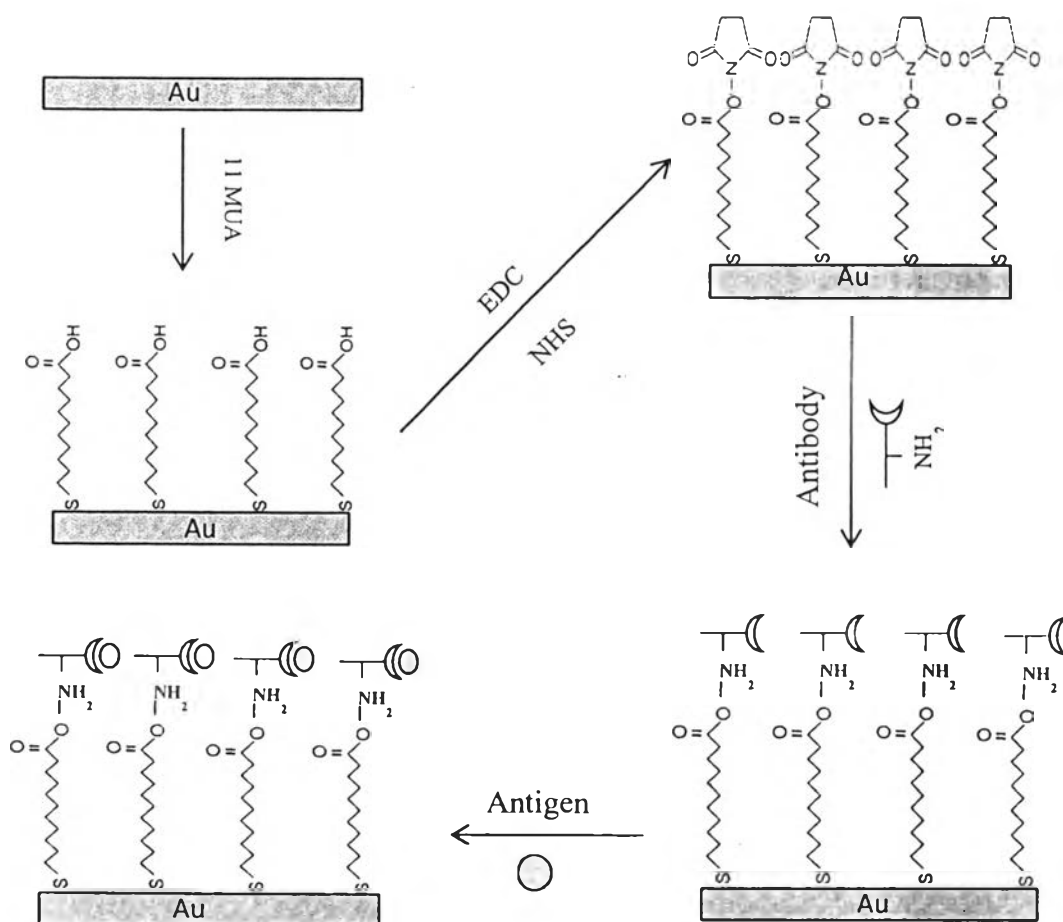

Figure 4.1 Schematic diagram of the fabrication of the biosensor.

First 11-mercaptoundecanoic acid (11MUA) was formed on a gold electrode through covalent bonding between the thiol group in 11MUA and gold. To maintain high sensitivity of sensing elements, it is important to find suitable linker compounds that enable sensing elements to be packed at a high density on the electrode surface. Therefore, the second step is the activation process of the SAM by formation of N-Hydroxysuccinimide (NHS) ester in the ethyl(dimethylaminopropyl) carbodiimide (EDC) solution, where the terminal carboxylic groups are converted to an active NHS esters (Ping *et al.*, 2008). After the activation of SAM in the NHS-EDC solution, the active NHS esters were replaced by the amines of antibody. Therefore the antibody was immobilized through amide bonding. Finally, a specific binding occurred between the immobilize antibodies and the antigens on the cell surface of Claudin 4 Recombinant protein during sensing process.

4.2 Cyclic Voltammetry Characterization

4.2.1 Cyclic Voltammetry of Gold Electrode After Each Assembly Step

Cyclic voltammetry is an important technique to evaluate the characteristics of electrochemistry. It provides useful information on changes of the properties of an electrode after each assembly step by using diffusion controlled redox couples as probes (Ganesh *et al.*, 2006). Figure 4.2 shows the cyclic voltammograms of bare gold and each assembly step in 0.1 M KCl, 5 mM $K_3Fe(CN)_6$ and 5 mM $K_4Fe(CN)_6 \cdot 3H_2O$ in 0.05 M phosphate buffer pH 7 as the supporting electrolyte with a potential scan rate 100 mV/s at room temperature. It reveals a reversible cyclic voltammogram at a bare gold electrode (Fig. 4.2a) indicating that the electron transfer was completely diffusion controlled (Ganesh *et al.*, 2006). After the bare gold electrode was covered with alkanethiol to generate a SAM, the permeability of SAM was so low that the redox probe could not penetrate in (Ping *et al.*, 2008) and therefore the response current decreased (Fig. 4.2b). Moreover, the penetration of the redox probe was reduced when Claudin 4 antibodies were immobilized on the gold SAM. Therefore, the magnitude of current response decreased (Fig. 4.2c). After the binding of Claudin 4 Recombinant proteins to the

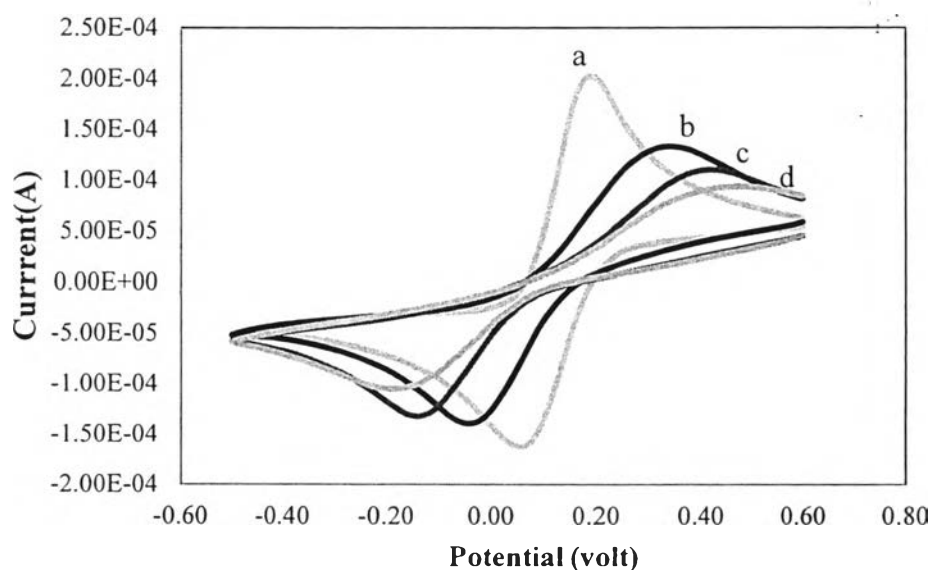immobilized antibodies, the penetration of the redox probe was further reduced (Fig. 4.2d)

Figure 4.2 Cyclic voltammetry in 0.1 M KCl, 5 mM $K_3Fe(CN)_6$ and 5 mM $K_4Fe(CN)_6 \cdot 3H_2O$ in 0.05 M phosphate buffer pH 7 as the electrolyte at the potential scan rate of 100 mV/s for (a) bare gold, (b) after formation of SAM, (c) after antibody immobilization, (d) after antigen binding.

4.2.2 Cyclic Voltammetry of Gold Electrode with Different Alkyl Chain Lengths of Alkanethiolate SAMs

Figure 4.3 shows the cyclic voltammograms of bare gold and SAMs with different alkyl chain lengths. It can be seen from Figure 4.3a that the bare gold exhibited a reversible peak for the redox couple indicating that the electron transfer rate was under the diffusion-controlled range. After the bare gold electrode was covered with the alkanethiols with different alkyl chain lengths, the redox probe could not penetrate deeply enough into the SAM, and thus the electron transfer was inhibited and, as a result, the response current decreased due to the high resistance from the SAM against electrons transferring through the SAM toward the gold surface (Hui *et al.*, 2005). It can also be seen that in the case of 11MUA (Fig 4.3e),

the CV result exhibited a significant resistance against electron transfer, which implies that a highly ordered, compact monolayer was formed on the gold surface. In contrast, a shorter chain length of alkanethiols showed the peak current values close to that of the bare gold electrode as shown in Figs. 4.3.b, c, and d. that the CV curves for 6MHA and 8MOA showed a moderate resistance against electron transfer. For 3MPA, the CV curve exhibited the lowest resistance against electron transfer as its peak current value is very close to that of the bare gold.
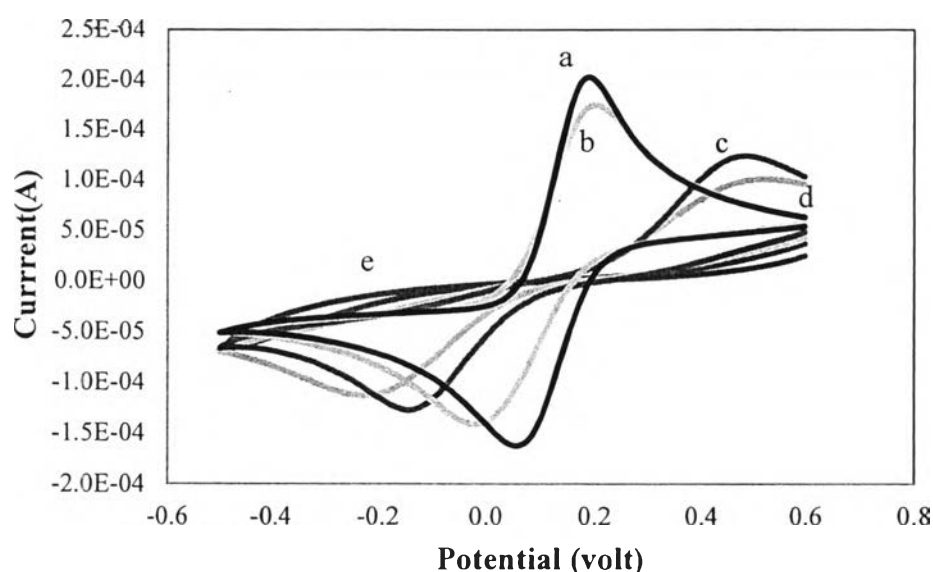
Figure 4.3 Cyclic voltammetry in 0.1 M KCl, 5 mM $K_3Fe(CN)_6$ and 5 mM $K_4Fe(CN)_6 \cdot 3H_2O$ in 0.05 M phosphate buffer pH 7 as the electrolyte at potential scan rate 100 mV/s for (a) bare gold, (b) 3MPA, (c) 6MHA, (d) 8MOA, (e) 11MUA.

4.3 Electrochemical Spectroscopy Impedance Characterization

4.3.1 Electrochemical Impedance Spectroscopy of Gold Electrode After Each Assembly Step

Electrochemical impedance spectroscopy (EIS) is a useful tool to characterize self-assembled monolayer on surfaces (Mouna *et al.*, 2008). A Nyquist diagram of electrochemical impedance spectroscopy is an effective way to measure

the electron transfer resistance. The inset box in Fig. 4.4 shows the EIS plot (Nyquist plot) of bare gold. The other curves for the each assembly step were obtained in a 0.05 M phosphate buffer solution at pH 7 with 0.1 M potassium chloride, 5 mM potassium ferricyanide and 5 mM potassium ferricyanide trihydrate .

The Nyquist plots represent two frequency regions. At high frequency, the semicircle part represents the charge transfer resistance that limits the electron transfer process. At lower frequency, the linear part is an electrochemical characteristic of a mass diffusion-limited electron transfer process (Park et al., 2011). It can be seen from the inset of Figure 4.4 that the bare gold electrode showed a low frequency straight line with a very small semicircle at high frequency region indicating a diffusion-controlled process for the redox couple on the bare gold surface. However, as shown in Figure 4.4a, b and c, after the deposition of each layer on the sensor surface, there was no linear part of the Nyquist plots and the diameter of the semicircle increased because the diffusion-controlled effect completely disappeared. This result showed that the layer deposition formed on the surface strongly hindered the electron transfer between the redox probe molecules and the surface of the electrode. This increase was due to the change of the electric characteristics of the gold/electrolyte interface (Mouna et al., 2008).
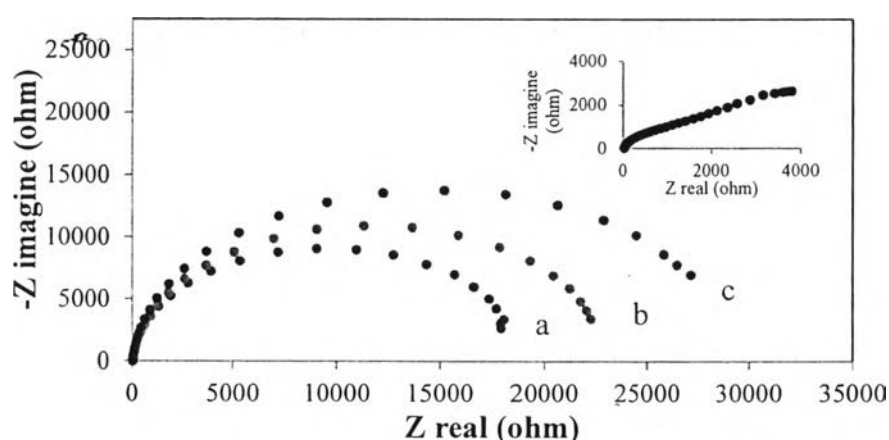

Figure 4.4 Impedance plot (Nyquist plot) in 0.1 M KCl, 5 mM $K_3Fe(CN)_6$ and 5 mM $K_4Fe(CN)_6 \cdot 3H_2O$ in 0.05 M phosphate buffer pH 7 as the supporting electrolyte for (a) after formation of SAM, (b) after antibodies immobilization, (c) after antigen binding, Inset shows the same impedance plot for bare gold .
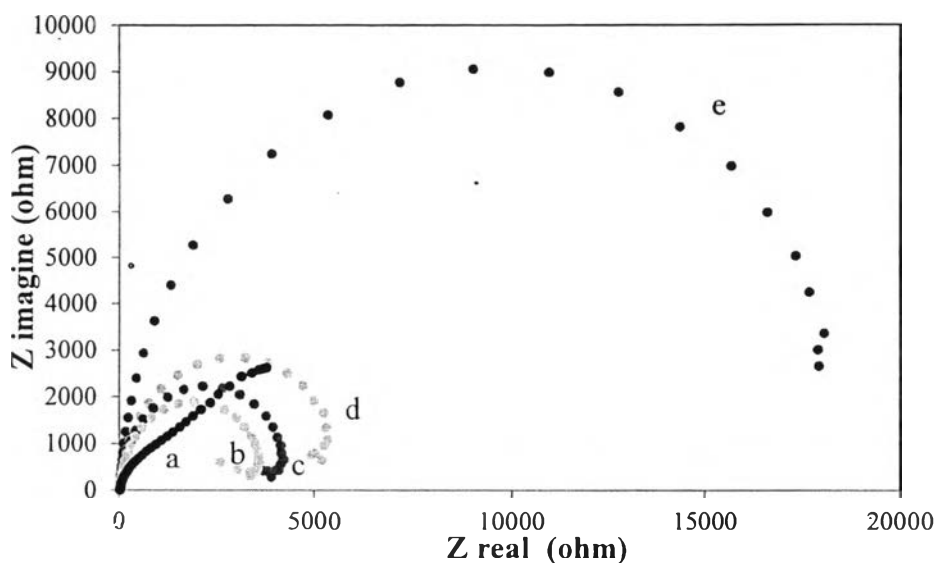
Figure 4.5 Impedance plot (Nyquist plot) in 0.1 M KCl, 5 mM $K_3Fe(CN)_6$ and 5 mM $K_4Fe(CN)_6 \cdot 3H_2O$ in 0.05 M phosphate buffer pH 7 as the supporting electrolyte for (a) bare gold, (b) 3MPA, (c) 6MHA, (d) 8MOA, (e) 11MUA.

4.3.2 Electrochemical Impedance Spectroscopy of Gold Electrode with Different Alkyl Chain Lengths of Alkanethiolate SAM

Figure 4.5 shows the EIS plots (Nyquist plot) of bare gold electrode and SAMs with different alkyl chain lengths. It can be seen from Fig. 4.5a that the Nyquist plot of bare gold showed a semicircle at high frequency region, which corresponded to the electron transfer limited process, followed by a linear part at low frequency region, indicating a diffusion-controlled process for the redox couple on bare gold. After the bare gold surface was cover by alkanethiols to form a SAM, then the EIS showed increases in the semicircle diameters in Nyquist plots of 3MPA (Fig. 4.3b), 6MHA (Fig. 4.3c), 8MOA (Fig. 4.3d), 11MUA (Fig. 4.3e). Because they showed large semicircles in the entire range of frequency, it is interpreted as a significant blocking of charge transfer and high resistance against electron transfer. This is because of the large insulating effect of alkanethiol (Mouna *et al.*, 2008). Comparing with the different alkyl chain lengths, a longer alkyl chain appears to provide more significant resistance against electron transfer to the redox probe than the short chains, possibly due to the increased travel distance for electrons and the

compactness between the polymers of SAMs that reduce the number of pinholes on the electrode surface.

4.3.3 Electrochemical Impedance Spectroscopy of the SAMs with Different Alkyl Chain Lengths After Immobilizing Antibodies and Binding Claudin 4 Recombinant Proteins
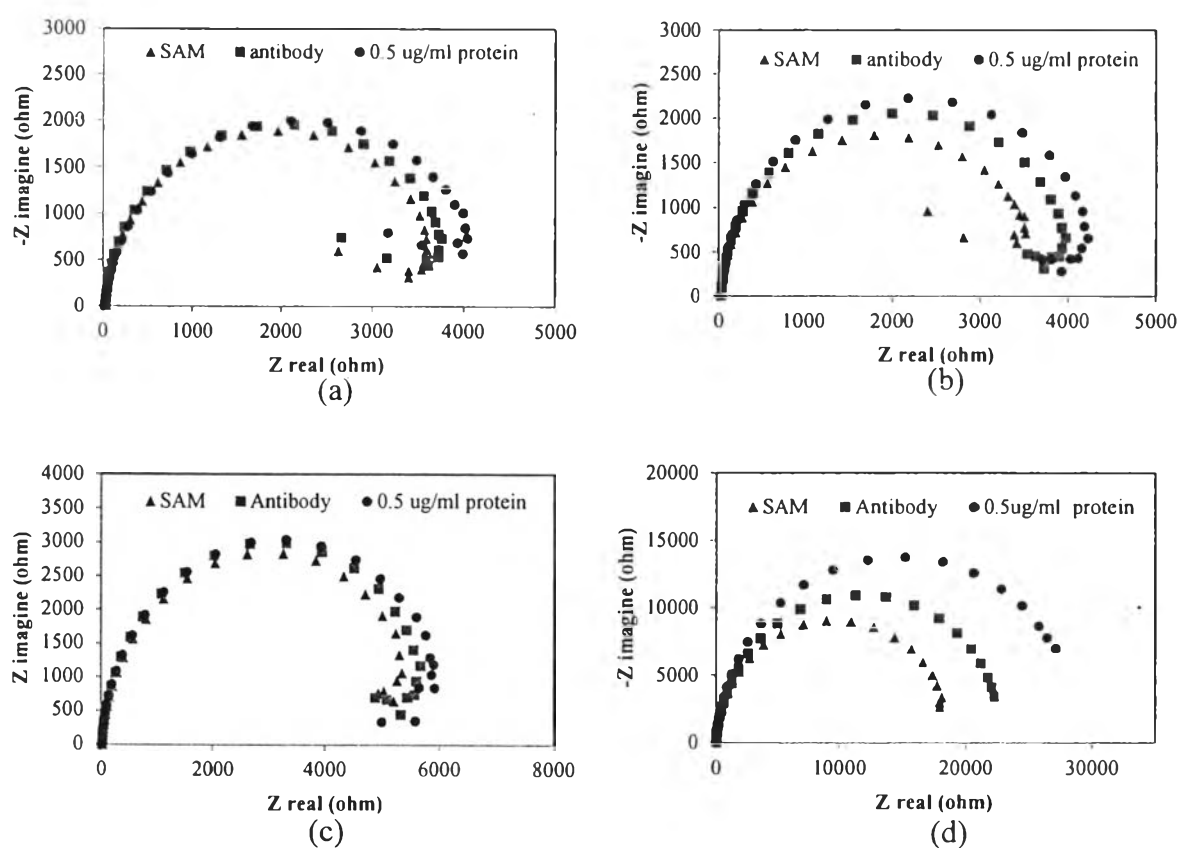

Figure 4.6 Impedance plot (Nyquist plot) of SAMs with different alkyl chain lengths after immobilizing antibodies and binding Claudin 4 Recombinant Proteins in 0.1 M KCl, 5 mM $K_3Fe(CN)_6$ and 5 mM $K_4Fe(CN)_6 \cdot 3H_2O$ in 0.05 M phosphate buffer pH 7 as the supporting electrolyte for (a) 3MPA (b) 6MHA, (c) 8MOA, (d) 11MUA.

Figure 4.6 shows the comparison of Nyquist diagrams of the SAMs with different alkyl chain lengths after immobilizing antibodies and binding Claudin 4 Recombinant Proteins. It can be seen that the SAMs of 3MPA, 6MHA, 8MOA and 11MUA showed the same trend of the Nyquist plots. After immobilizing antibodies and binding Claudin 4 Recombinant Proteins, as shown in Figure 4.5a, b, c and d, there were no the linear parts of the Nyquist diagrams and the diameters of the semicircles increased. These results indicate that the diffusion-controlled effect completely disappeared. These results showed that the each layer deposition formed on the surface strongly blocked the electron transfer between the redox probe and the surface of the electrode. In the case of 11MUA, it generated larger signal than others indicating a stronger blocking against electron transfer.

4.4 Detection of Claudin 4 Recombinant Proteins Using Electrochemical Impedance Spectroscopy

A Nyquist diagram of electrochemical impedance spectroscopy is an effective way to measure the electron transfer resistance. Figure 4.7 shows the representative Nyquist diagrams of the sensor reacted with different concentrations of Claudin 4 Recombinant Protein. Curves a-d represent the Claudin 4 Recombinant Protein concentration of 0 μg/ml, 0.5 μg/ml, 1 μg/ml, 2 μg/ml, respectively. It can be seen from Fig. 4.7 that the semicircle diameters in the Nyquist plots increased with the Claudin 4 Recombinant Protein concentration. Furthermore, there were no linear parts in the Nyquist diagrams verifying that as the Claudin 4 Recombinant Proteins bounded to the sensor, the electron transfer resistance increased. It is thought that the bounded proteins provided stronger resistance against electron transfer to the redox probe.
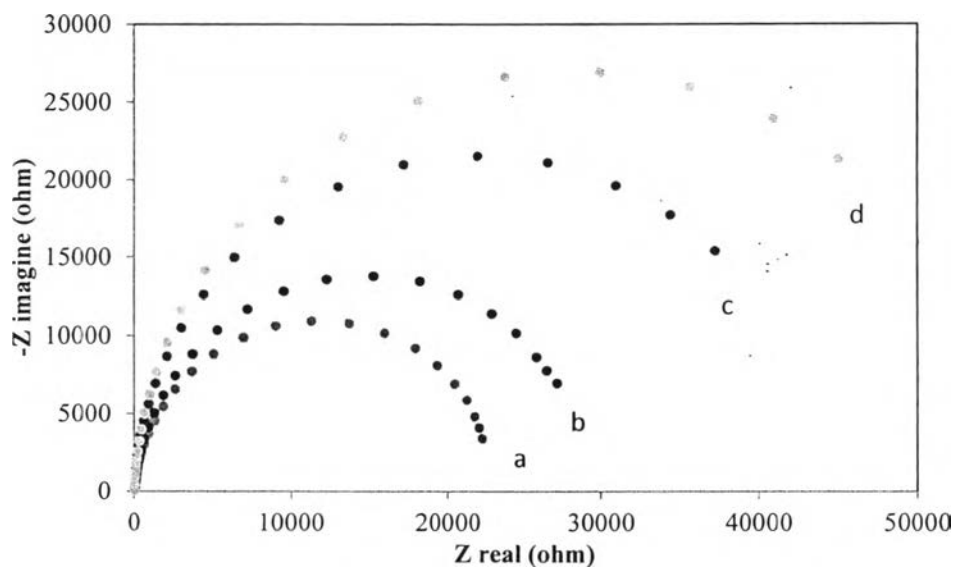
Figure 4.7 Impedance plot (Nyquist plot) of the sensor with different concentrations of Claudin 4 Recombinant Proteins in 0.1 M KCl, 5 mM $K_3Fe(CN)_6$ and 5 mM $K_4Fe(CN)_6 \cdot 3H_2O$ in 0.05 M phosphate buffer pH 7 as the supporting electrolyte for (a) 0 μg/ml (b) 0.5 μg/ml, (c) 1 μg/ml, (d) 2 μg/ml.